Computers and Chemical Engineering 114 (2018) 254–264

Contents lists available at ScienceDirect

Computers and Chemical Engineering

journal homepage: www.elsevier.com/locate/compchemeng

Economic opportunities for industrial systems from frequency regulation markets

Alexander W. Dowling, Victor M. Zavala*

Department of Chemical and Biological Engineering, University of Wisconsin-Madison, 1415 Engineering Dr, Madison, WI 53706, USA

ARTICLE INFO

Article history:
Received 15 June 2017
Received in revised form 2 September 2017
Accepted 21 September 2017
Available online 23 September 2017

Keywords:
Electricity markets
Frequency regulation
Dynamics
Manufacturing
Control

ABSTRACT

We analyze economic opportunities for industrial facilities provided by frequency regulation (FR) markets. We use classical frequency domain analysis techniques to characterize the harmonic content of FR signals and to analyze the impact of such harmonics on the response of dynamical systems. The analysis reveals that systems with slow dynamics, as those found in large industrial facilities, are suitable to provide FR capacity because they can naturally damp the dominant high-frequency harmonic content of FR signals. We also propose optimization formulations to quantify the maximum amount of FR capacity that can be provided by a system given its dynamic characteristics, its control architecture. A distillation case study demonstrates that significant economic potential exists for large industrial facilities.

1. Introduction

Electricity markets are hierarchical decision-making processes that seek to coordinate generation, transmission, and consumption resources at multiple timescales. Fig. 1 shows the major market layers, products, and timescales for the California Independent System Operator (CAISO). These markets exchange two general types of products: electrical energy and ancillary service capacity. Electrical energy is sold at three different timescales: in the Day-Ahead Market (DAM) with 1-h intervals, in the Fifteen-Minute Market (FMM) with 15-min intervals, and in the Real Time Dispatch Process (RTPD) with 5-min intervals. The FMM and RTPD layers are also known as the Real-Time Market (RTM). The process of determining the resource dispatch schedule and locational (nodal) prices from bids is known as market clearing. Market clearing for the DAM occurs around noon of each preceding day. The RTM market corrects for errors in the original DAM schedule (which often arise from forecasting inaccuracies). As a result, RTM prices are more violative and provide economic opportunities for market participants with dynamic (ramping) flexibility (Dowling et al., 2017). Electricity markets across the U.S. include both DAM and RTM processes but layer names, timescales, and specific rules may vary by region.

In addition to energy products, resources can also provide flexibility in the form of *ancillary services* such as frequency regulation, spinning reserves, and non-spinning reserves. In contrast to energy transactions (with prices in $/MWh), ancillary services are a contingency product, where resources are paid for providing power capacity (with price in $/MW). Reserve capacities provide a contingency in the event of unforeseen events that cannot be met by RTM (e.g., wind and solar supply variations and generator failures). For example, a resource providing *spinning reserves* in CAISO is contractually obligated to fully respond within 10 min of dispatch and provide 30–60 min of power at the awarded reserve capacity. Requirements for *non-spinning reserves* are less stringent, which allows resources with less dynamic flexibility to participate. Dispatch of reserves is rare; for example, Alcoa reported 55 dispatches of reserves per year for a facility providing interruptible loads (similar to reserve capacity) in the Midcontinent ISO (Todd et al., 2009; Todd, 2013).

The *frequency regulation* (FR) ancillary service helps balance the grid on the seconds to minutes timescales. As the name suggests, FR is needed to keep the frequency of the grid at a required level (60 Hz in the U.S.). Resources providing FR capacity offer a *flexibility band* to the market. Every 2–15 s, the Automatic Generator Control (AGC) system sends each resource providing FR capacity a new power set-point (FR dispatch signal) within the flexibility band. Each resource is compensated for both the size of the band (i.e., the capacity provided in MW) and also for the amount of variability in the FR dispatch signal. The variability is known as *mileage* and is defined as the absolute distance between consecutive power set-points. Fig. 2 shows the set-point and mileage for a hypothetic generator providing FR capacity. The flexibility band is split into regulation up and regulation down capacities, which are priced separately in some markets such as CAISO and the Electric Reliability

* Corresponding author.
E-mail address: victor.zavala@wisc.edu (V.M. Zavala).

https://doi.org/10.1016/j.compchemeng.2017.09.018
0098-1354/

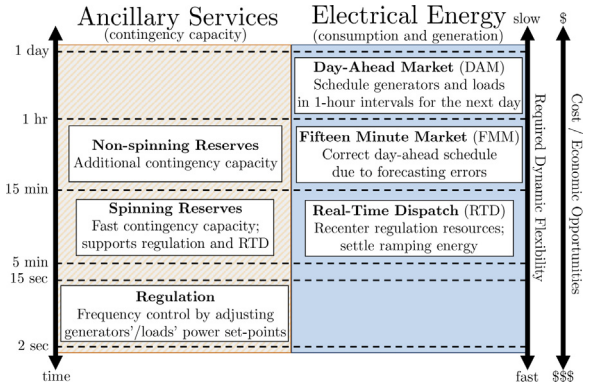

Fig. 1. Market-based control hierarchy for the power grid. Resources may participate via multiple ancillary service and energy products (Dowling et al., 2017).

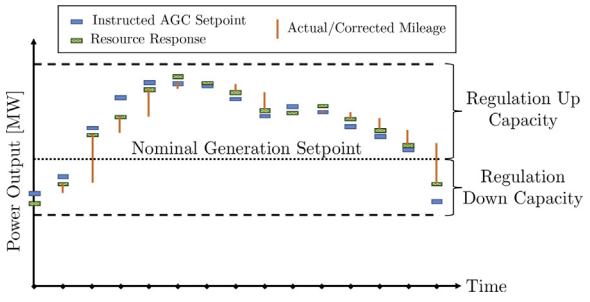

Fig. 2. Illustration of FR dispatch signal, flexibility (capacity), and mileage (Dowling et al., 2017).

Council of Texas (ERCOT). The nominal set-point is the scheduled power output as set by an energy market (e.g., DAM). Compared to reserves, providing FR capacity requires *significantly more dynamic flexibility* from generators and loads. As a result, FR capacity is the most expensive ancillary service (by a factor of two or more compared to reserves). For example, in the case of CAISO for the year of 2015, the average FR capacity price was $ 5.72/MW, compared to $2.84/MW and $0.30/MW for spinning and non-spinning reserve capacity, respectively.

Several industrial facilities already exploit economic opportunities from electricity markets. For example, in ERCOT, load resources provide 2400 MW of flexible capacity, including over half of the spinning reserves. Notably, over 1000 MW of this capacity is provided by a single electrochemical manufacturing facility. Of the remaining capacity, 820 MW and 520 MW are provided by medium (10–50 MW) to small (less than 10 MW) industrial and commercial loads, respectively. In the year of 2015, a load could have saved 400,000 $/yr in CAISO by shifting 10 MW of consumption from during the 1% most extreme RTM prices (between 97 and 1621 $/MWh) to the average price (30 $/MWh). Similarly, a load providing 10 MW of FR capacity for every hour would have received 500,000 $/yr in capacity payments (Dowling et al., 2017).

The demand and prices for ancillary services is increasing, driven by high frequency variations of non-dispatchable renewable resources (e.g., solar, wind) (Walling, 2008; Kirby et al., 2011; Mullin, 2016). In light of these economic opportunities, single sites often participate in multiple demand response (DR) programs and ISO markets. For example, Alcoa's aluminum smelter in Warrick, IN provides 70 MW of FR capacity to the Midcontinent ISO market. This represents 15% of the average load (470 MW) for the system. The same facility also provides 75 MW of interruptible load (a separate DR program) (Todd et al., 2009; Todd, 2013). According to the Energy Information Administration (EIA), the U.S. industry consumed 846 TWh of electricity in 2010, with 71.7% of the demand arising from six major sectors: chemicals (22.1%), primary metals (14.5%), paper (12.2%), food (9.6%), petroleum and coal products (7.8%), and plastics and rubber products (5.4%) (Table 11.1 EIA, 2013). A recent analysis of CAISO data revealed substantial economic opportunities for industrial systems that can provide flexibility at fast timescales (RTM and FR) (Dowling et al., 2017). For example, for battery and CHP systems, it has been found that 60–90% of potential revenues are only accessible through RTM. Similarly, providing ancillary services can increase revenues 40–100% relative to only transacting energy. Consequently, the ISOs can greatly benefit from more active participation of these sectors in electricity markets.

Applications for industrial demand response include combined heat and power (CHP) utility plants (Rong and Lahdelma, 2007; Al-Mansour and Kožuh, 2007; De Paepe and Mertens, 2007; Christidis et al., 2012; Mitra et al., 2013; Coatalem et al., 2017; Feng et al., 2015), steel furnaces (Ashok, 2006; Castro et al., 2013), cement plants (Castro et al., 2011, 2009; Mitra et al., 2012; Coatalem et al., 2017; Vujanic et al., 2012), air separation units (Cao et al., 2015, 2016; Ierapetritou et al., 2002; Mitra et al., 2012; Pattison et al., 2016; Zhang et al., 2015a, 2016b; Zhu et al., 2011, 2011; Karwan and Keblis, 2007; Zhou et al., 2017), electrochemical manufacturing facilities (Babu and Ashok, 2008), and pulp mills (Everett and Philpott, 2002). Early literature focused on augmenting production scheduling frameworks to incorporate time-varying energy prices (Daryanian et al., 1989; Ashok and Banerjee, 2001). Initial extensions considered uncertain future energy prices using stochastic programming formulations (Ierapetritou et al., 2002; Everett and Philpott, 2002). More recent work also considered uncertain product demands (Zhang et al., 2016a) as well as robust optimization formulations (Vujanic et al., 2012; Zhang et al., 2016b, 2015a). Time is typically discretized into one-hour or longer intervals that correspond with prices from DAM or time-of-day pricing schemes in one-day or one-week planning horizons (Zhang and Grossmann, 2016). All of these modeling approaches assume steady-state operation and thus neglect process dynamics. Although this is a reasonable assumption for participation in DAM, dynamics are essential for ancillary services operating at faster timescales. As such, multiscale modeling approaches are becoming increasingly relevant.

Different approaches have been proposed to incorporate process dynamics into production scheduling models, with cryogenic air separation units (ASUs) being one of the most relevant applications (Zhang et al., 2015a, 2016b; Cao et al., 2016; Pattison et al., 2016). These systems produce purified oxygen, nitrogen, and argon by distillation with two or three mass and heat integrated columns. The separation is energy intensive due to the refrigeration needs, with compressor electrical loads reaching levels of up to 100 MW for large systems. As such, important economic opportunities from RTM and FR markets are available for these systems. Unfortunately, a common perception in the chemical industry is that systems exhibiting slow dynamics such as ASUs (time constants on the order of several hours) are not suitable for RTM and FR markets because they will not be able to track fast-varying dispatch signals. The majority of ancillary service capacity, however, is in fact provided by large equipment units such as aluminum smelters (Zhang and Hug, 2014, 2015) and electric arc furnaces (Zhang et al., 2015b). This is because these systems can absorb fast variations in electrical energy input with negligible impact on product quality. In other words, in these systems *FR signals are treated as disturbances and not as tracking signals*.

An increasing share of ancillary service capacity is provided by energy storage technologies, such as batteries, that can provide power within less than a second (Fares et al., 2014). Because the flexibility of these systems is well known, literature focuses on bidding strategies under uncertainty and simultaneous provision

of multiple products. To this effect, we recently proposed an optimization framework for participation in multiple product markets (energy and ancillary services) at multiple timescales (day-ahead and real-time) (Dowling et al., 2017). Several recent studies explore providing ancillary services from building heat and cooling systems (Hao et al., 2012; Zhao et al., 2013, 2015; Baccino et al., 2014). In one study, Lin et al. (2015) demonstrate the feasibility of modulating fan power consumption at fast frequencies (10^{-2}–10^{-3} Hz) to provide FR capacity while not disturbing chiller operation (10^{-4} Hz and slower). A recent study has also explored the possibility of coordinating millions of pool pumps in Florida to provide FR capacity at a large scale (Meyn et al., 2013).

In this work, we explore the ability of traditional chemical processes such as distillation towers, pipelines, and cooling towers to also participate in frequency regulation markets by exploiting flexibility from mechanical equipment, pumps, fans, electric heaters, or steam supply (from CHP generation). The withstanding question is, however, *to what extent can chemical processes tolerate high-frequency electrical load fluctuations*? In order to address this question, we use classical frequency domain analysis techniques to characterize the harmonic content of FR signals and to analyze the impact of such harmonics on the response of dynamical systems. The results illustrate that systems with slow dynamics, as those found in large chemical processes, are suitable to provide FR capacity because they can naturally damp the dominant high-frequency harmonic content of FR signals. We also propose simple and rigorous data-driven strategies to quantify the maximum amount of FR capacity that can be provided by a given system given its dynamic characteristics, its control structure, and FR dispatch signals. A simple first-order system and a distillation case study demonstrate that significant economic potential exists for large industrial systems.

The paper is organized as follows. Section 2 reviews classical frequency domain analysis techniques to analyze the response of a given dynamical system to harmonic signals. Section 3 analyzes the frequency spectrum of FR signals and prices from historical data from ERCOT and CAISO markets. Section 4 presents an optimization formulation to determine the maximum FR capacity that a given dynamical system can provide. Section 5 provides case studies to illustrate the concepts while Section 6 outlines conclusions and future work.

2. Frequency domain analysis

We begin by analyzing the response of a dynamical system to harmonic signals. We use the following scalar system in the frequency domain:

$$y(j\omega) = H(j\omega)d(j\omega) \tag{2.1}$$

where $\omega \in \mathbb{R}$ is the frequency, $j := \sqrt{-1} \in \mathbb{C}$, $d(j\omega) \in \mathbb{C}$ is the input disturbance, $y(j\omega) \in \mathbb{C}$ is the output, and $H : \mathbb{C} \to \mathbb{C}$ is the transfer function. We recall that the transfer function can be expressed as a phasor $H(j\omega) = |H(j\omega)|e^{\angle H(j\omega)}$ or in rectangular form $H(j\omega) = \Re H(j\omega) + j \cdot \Im H(j\omega)$. It is well-known that the response of a stable system $H(j\omega)$ (i.e., with stable poles) to a sinusoidal input settles at a sinusoidal steady-state known as the ultimate period response (UPR) (Babatunde and Ray, 1994; Cusset and Mellichamp, 1975). To see this, we recall that the ultimate system response can be expressed in the time domain by using the convolution form:

$$\hat{y}(t) = \int_0^\infty h(\tau)d(t-\tau)d\tau \tag{2.2}$$

where $h : \Re \to \Re$ is the inverse Laplace transform of $H(\cdot)$. If we define $d(t) = A \cdot \sin(\omega t)$ (where $A \in \mathbb{R}$ is the amplitude of the input signal) and recall from Euler's identities that $\sin(\omega t) = \frac{1}{2j}(e^{j\omega t} - e^{-j\omega t})$, we can establish that:

$$\begin{aligned}
\hat{y}(t) &= \int_0^\infty h(\tau)A\sin(\omega(t-\tau))d\tau \\
&= \frac{A}{2j}\int_0^\infty h(\tau)(e^{j\omega t} - e^{-j\omega t})d\tau \\
&= \frac{A}{2j}\int_0^\infty h(\tau)e^{j\omega t} - \frac{A}{2j}\int_0^\infty h(\tau)e^{-j\omega t}d\tau \\
&= \frac{A}{2j}e^{j\omega t}H(j\omega) - \frac{A}{2j}e^{-j\omega t}H(-j\omega) \\
&= \frac{A}{2j}e^{j\omega t}(\Re H(j\omega) + j\Im H(j\omega)) - \frac{A}{2j}e^{-j\omega t}(\Re H - j\Im H(j\omega)) \\
&= \frac{A}{2j}\Re H(e^{j\omega t} - e^{-j\omega t}) + \frac{A}{2}\Im H(e^{j\omega t} + e^{-j\omega t}) \\
&= A\Re H\sin(\omega t) + A\Im H\cos(\omega t) \\
&= A|H(j\omega)|\sin(\omega t + \angle H(j\omega))
\end{aligned}$$

In other words, the UPR is a sinusoidal response with amplitude $A|H(j\omega)|$ and phase $\angle H(j\omega)$. Similarly, if we define the disturbance signal $d(t) = A \cdot \cos(\omega t)$ and recall that $\cos(\omega t) = \frac{1}{2}(e^{j\omega t} + e^{-j\omega t})$, we can establish that:

$$\begin{aligned}
\hat{y}(t) &= \int_0^\infty h(\tau)A\cos(\omega(t-\tau))d\tau \\
&= \frac{A}{2}\int_0^\infty h(\tau)(e^{j\omega t} + e^{-j\omega t})d\tau \\
&= \frac{A}{2}\int_0^\infty h(\tau)e^{j\omega t} + \frac{A}{2}\int_0^\infty h(\tau)e^{-j\omega t}d\tau \\
&= \frac{A}{2}e^{j\omega t}H(j\omega) + \frac{A}{2}e^{-j\omega t}H(-j\omega) \\
&= \frac{A}{2}e^{j\omega t}(\Re H(j\omega) + j\Im H(j\omega)) + \frac{A}{2}e^{-j\omega t}(\Re H - j\Im H(j\omega)) \\
&= \frac{A}{2}\Re H(e^{j\omega t} + e^{-j\omega t}) + \frac{A}{2}j\Im H(e^{j\omega t} - e^{-j\omega t}) \\
&= A\Re H\cos(\omega t) - A\Im H\sin(\omega t) \\
&= A|H(j\omega)|\cos(\omega t + \angle H(j\omega))
\end{aligned}$$

For any disturbance signal of the form

$$d(t) = \sum_{k=0}^{N}(A_k\sin(\omega_k t) + B_k\cos(\omega_k t)), \tag{2.3}$$

where $A_k \in \mathbb{R}$ and $B_k \in \mathbb{R}$ are the amplitude coefficients corresponding to frequency $\omega_k \in \mathbb{R}$, we have that the UPR is given by:

$$\hat{y}(t) = \sum_{k=0}^{N}|H(j\omega_k)|\left(A_k\sin(\omega_k t + \angle H(j\omega_k)) + B_k\cos(\omega_k t + \angle H(j\omega_k))\right). \tag{2.4}$$

Consequently, the UPR can be expressed as a sum of harmonics covering a given frequency spectrum.

For a first-order system of the form $H(j\omega_k) = \frac{K}{\tau(j\omega_k)+1}$, with gain $K \in \mathbb{R}$ and time constant $\tau \in \mathbb{R}_+$, we have that:

$$|H(j\omega_k)| = \frac{|K|}{\sqrt{(\omega_k\tau)^2 + 1}} \tag{2.5a}$$

$$\angle H(j\omega_k) = -\tan^{-1}\omega_k\tau. \tag{2.5b}$$

We can thus see that for a system with *fast dynamics* (i.e., $\tau \to 0$) we have that $|H(j\omega_k)| \to |K|$ while for a system with slow dynamics (i.e.,

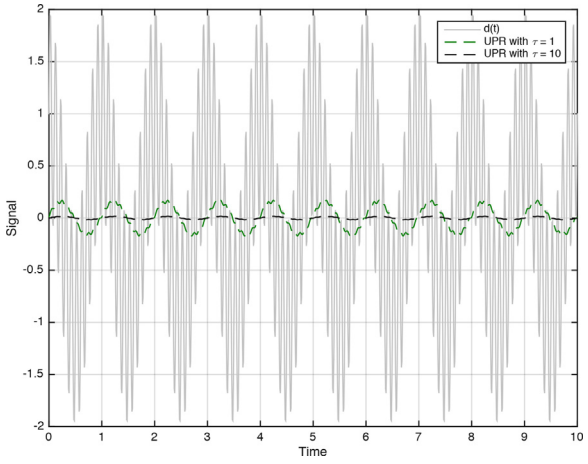

Fig. 3. UPR for a fast and slow first-order system.

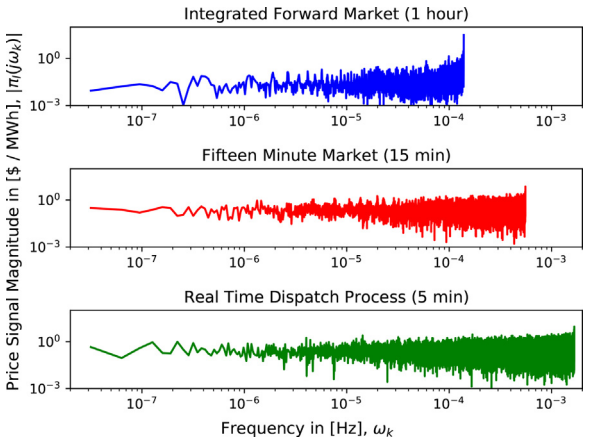

Fig. 4. Frequency spectrum for CAISO energy prices near Daggett, CA in 2015.

$\tau \to \infty$) we have $|H(j\omega_k)| \to 0$. In other words, as the *system becomes slower, it naturally damps the disturbance signal* (the amplitude of the UPR becomes smaller). If we interpret the origin as a given reference steady-state, this indicates that a slower system will exhibit small deviations from the reference point even in the face of a strong disturbance signal. We also note that a system with a given time constant τ is strongly affected by frequencies ω_k smaller than $\mathcal{O}(\tau^{-1})$. Consequently, if τ is large (say $\mathcal{O}(10)$) and the harmonic content of a disturbance signal is dominated by frequencies larger than $\mathcal{O}(\tau^{-1})$ (measured in terms of the magnitude coefficients A_k and B_k), we can expect the dynamical system to be rather insensitive to the disturbance. These concepts are illustrated in Fig. 3, where we present the UPR of a first-order system with two different time constants ($\tau = 1$ and $\tau = 10$) to a disturbance composed of two harmonics ($\omega_1 = 1$ and $\omega_1 = 10$). Note that the slower system with $\tau = 10$ damps the harmonics more strongly.

3. Analysis of market data

ISOs generate and disclose enormous amounts of market data. For example, CAISO generates over *1 trillion price data points each year*, all of which are available through oasis.caiso.com. This data volume reflects the underlying complexity of market operations. In particular, energy prices are set at three timescales (1-h, 15-min, 5-min intervals) and vary spatially due to the transmission network topology. The CAISO system contains over 8000 nodes and each node has three locational marginal prices for energy at every instance in time (one for each market layer). In contrast, ancillary service prices are often set for a few regions (hubs) or are spatially uniform for the entire network. In addition to prices, ISOs often release aggregate bid data, network information (nodes type, name, GPS coordinates), and historical FR dispatch signals. As we show next, when combined with system engineering techniques, these datasets can offer valuable insights for industrial market participants on economic potential of market participation and for ISOs on incentives provided by market signals.

To identify the potential of an industrial dynamical system to participate in electricity markets, we begin by identifying the dominant timescales in the market signals. To do this, we represent market price signals, $\pi(t)$, using Fourier expansions of the form:

$$\pi(t) = \sum_{k=0}^{N} A_k \sin(\omega_k t) + B_k \cos(\omega_k t), \tag{3.6}$$

The magnitude of the corresponding frequency domain signal at frequency ω_k is given by:

$$|\pi(j\omega_k)| = \sqrt{A_k^2 + B_k^2}. \tag{3.7}$$

Fig. 4 shows the frequency spectrum of historical IFM, FFM, and RTPD energy prices near Daggett, CA in 2015. We have found that, in all three markets, 97% of the total signal magnitude (given by $\sum_{k=0}^{N} |\pi(j\omega_k)|$) arises from frequencies larger than 10^{-5} Hz (which correspond to day-to-day variations). Most notably, 60% of the total magnitude of IFM price signal (15-min price intervals) and 95% of the total magnitude of the RTPD price signal (5-min price interval) arises from frequencies smaller than 10^{-4} Hz (which corresponds to 2.75 h periods). This illustrates that industrial systems seeking to participate in these energy markets must be capable of adjusting electrical loads at similar timescales.

Industrial systems seeking to provide FR capacity must also be concerned with dynamics of the FR dispatch signal. ERCOT currently discloses historical FR dispatch signals for the first eleven days of each month from July 2015 to June 2016.[1] These datasets include the system-wide dispatch signal and the total available FR capacity (both in MW) for regulation up and down products. We use $\beta_+(t) \geq 0$ and $\beta_-(t) \geq 0$ to represent the regulation up (RU) and regulation down (RD) dispatch signals, respectively, which are expressed as a fraction of the available capacity. Note that these signals are mutually exclusive (i.e., $\beta_+(t) \cdot \beta_-(t) = 0$). Similar to the case of price signals, the harmonic content of the *total FR dispatch signal* $\beta(t) = \beta_+(t) - \beta_-(t)$ can be obtained by using a Fourier expansion. Fig. 5 shows the FR signal for ERCOT in year 2016 both as a time series and decomposed into its harmonic components. This ISO updates individual resource electrical power set-points every 4 s (0.25 Hz). We have found that approximately *70% of the total magnitude of the FR dispatch signal arises from frequencies between 10^{-2} Hz (1.7 min period) and 10^{-4} Hz (16.7 min period).* This indicates that, in principle, *chemical processes can absorb most of the harmonic content of FR dispatch signals* because equipment usually have time constants on the order of minutes to hours. Moreover, industrial systems are usually equipped with robust control architectures (e.g., real-time optimization, model predictive control, and regulatory control) that are designed to suppress a wide variety of disturbances.

Another key question is whether mileage payments are important in FR markets. Recall that resources providing FR are compensated for both capacity (size of the flexibility band) and

[1] http://www.ercot.com/mktrules/pilots/frrs.

Table 1
Summary of FR capacity and mileage prices in CAISO during 2015. RD and RU stand for regulation down and up, respectively. Data obtained from oasis.caiso.com.

	Quantile					
	0.0	0.2	0.4	0.6	0.8	1.0
RD capacity price ($/MW cap.)	0.0	1.74	2.62	3.27	3.91	58.88
RD miles amount (MW miles/MW cap.)	0.0	2.07	3.9	5.74	8.53	32.68
RD miles price ($/MW miles)	0.0	0.01	0.01	0.01	0.1	6.83
RD miles revenue ($/MW cap.)	0.0	0.02	0.06	0.11	0.44	12.56
RU capacity price ($/MW cap.)	0.0	1.55	2.23	3.99	7.84	55.24
RU miles amount (MW miles/MW cap.)	0.0	0.25	0.97	2.53	4.75	30.99
RU miles price ($/MW miles)	0.0	0.0	0.0	0.01	0.01	37.26
RU miles revenue ($/MW cap.)	0.0	0.0	0.0	0.02	0.06	92.62

mileage. The latter accounts for the variability of the FR dispatch signal. Table 1 shows regulation capacities prices, mileage amounts, mileage prices, and mileage revenues for the CAISO DAM market (1-h intervals). CAISO only releases the average mileage for each hour per unit of FR capacity. Using these data, we compute the anticipated revenue from mileage. Table 1 reports quantiles to summarize the distributions of each quantity over the year. We see that, between the 0.0 and 0.6 quantiles, mileage revenue is less than 3% of the overall capacity revenue. At the highest prices and mileage dispatch (1.0 quantile), mileage revenues become significant. These results indicate that neglecting mileage payments will not incur a large penalty. It is important to highlight, however, that this conclusion is based on the average mileage allocation.

4. Optimal frequency regulation provision

Our goal is to quantify the maximum amount of FR capacity that a system can provide in order to maximize FR revenue and while maintaining operational constraints (safety bounds, set-point deviations, product quality, wear-and-tear, and so on). We do this by posing an optimization problem of the form:

$$\min_{r_+(\cdot),r_-(\cdot),u(\cdot)} \int_{\mathcal{T}} \phi(z(t),u(t),d(t))dt \tag{4.8a}$$

$$\text{s.t. } \dot{z}(t) = f(z(t),u(t),d(t)),\ t \in \mathcal{T} \tag{4.8b}$$

$$y(t) = h(z(t)),\ t \in \mathcal{T} \tag{4.8c}$$

$$g(z(t),y(t),u(t)) \le 0,\ t \in \mathcal{T} \tag{4.8d}$$

$$d(t) = r_+(t)\beta_+(t) - r_-(t)\beta_-(t),\ t \in \mathcal{T} \tag{4.8e}$$

$$0 \le r_+(t), r_-(t) \le \alpha,\ t \in \mathcal{T}. \tag{4.8f}$$

where $\mathcal{T}$ is the time domain, $z(t) \in \mathbb{R}^{n_z}$ are the states at time t, $y(t) \in \mathbb{R}^{n_y}$ represents the outputs, $u(t)$ are the controls, and $d(t)$ are the disturbances. We highlight that this formulation is general and considers multivariable dynamical systems. For simplicity, we assume that the only disturbance affecting the system is the FR dispatch signal. The constraints (4.8d) capture operational limits; for instance, an operator might be interested in imposing constraints on the maximum deviation of a system output $y(t)$ from a given desired steady-state $\bar{y}$ of the form:

$$\|y(t) - \bar{y}\| \le \epsilon,\ t \in \mathcal{T}, \tag{4.9}$$

where $\epsilon \in \mathbb{R}_+$ is a *flexibility margin* that measures the maximum allowable deviation (where $\|\cdot\|$ is any suitable norm). The FR dispatch signal $d(t)$ is decomposed into its FR up component $\beta_+(t) \in \mathbb{R}_+$ and its FR down component $\beta_-(t) \in \mathbb{R}_+$. Although the harmonic content of the FR signal is fixed, the operator can manipulate its magnitude by adjusting the amount of FR up and down capacity provided to the market, which is represented by the variables $r_+(t) \in \mathbb{R}_+$ and $r_-(t) \in \mathbb{R}_+$. These capacities are bounded by the parameter $\alpha \in \mathbb{R}_+$. The objective function $\phi(\cdot)$ captures revenue from the FR market and other operational costs. The revenue collected from FR capacity is simply $\int_{\mathcal{T}}(\pi_+(t)r_+(t) + \pi_-(t)r_-(t))dt$ where $\pi_+(\cdot), \pi_-(\cdot)$ are the prices for regulation up and down capacity, respectively. The prices $\pi_+(t), \pi_-(t)$ and capacities $r_+(t), r_-(t)$ are piece-wise (zero-hold) trajectories where the length of the zero-hold period is one hour. The FR revenue can also potentially capture mileage payments but we do not explore this aspect in this work because FR capacity is the most dominant revenue item.

In summary, the goal of the proposed optimization formulation is to determine optimal trajectories $r_+(t), r_-(t), u(t),\ t \in \mathcal{T}$ that maximize the system economic objective function while satisfying the constraints. Note that $d(\cdot)$ acts as a disturbance and the system is remunerated for its ability to counteract such disturbance by using the controls $u(\cdot)$. Consequently, the more flexibility the control system has to counteract disturbances, the more FR revenue that can potentially be collected.

5. Case studies

5.1. First-order system

We first illustrate some of the concepts discussed by using an open-loop first-order system. This seeks to highlight the interplay between the system dynamics, process flexibility, and FR revenue. This analysis also gives a quick approach to estimate the FR revenue for a given first-order system. A more sophisticated procedure for general dynamical systems is presented in Section 5.2.

Consider an input signal of the form $d(t) = r \cdot A \cdot \sin(\omega t)$, where ω and A are known parameters that denote the frequency and amplitude of the FR signal. The ISO pays the industrial facility for the FR capacity $r \in \mathbb{R}_+$ at price $\pi \in \mathbb{R}_+$ (same price for FR up and down capacity). We thus seek to find r that maximizes the revenue $\phi(r) = \pi \cdot r$ while keeping the magnitude of the UPR bounded as $r \cdot A \cdot |H(j\omega)| \le \epsilon$. Here, ϵ is a *flexibility margin* that captures the maximum allowable deviation from a given steady-state. Since the UPR is symmetric and periodic, the UPR bound can also be written in the time domain as $\max_{t \in \mathcal{U}} |\hat{y}(t) - \bar{y}| \le \epsilon$, where $\hat{y}(t)$ is the UPR and $\mathcal{U}$ is the period of oscillation of the UPR.

The FR revenue maximization problem can thus be written as:

$$\max_r \ \pi \cdot r \tag{5.10}$$

$$\text{s.t. } \frac{r \cdot A \cdot |K|}{\sqrt{(\omega\tau)^2 + 1}} \le \epsilon. \tag{5.11}$$

Since r enters linearly in the objective and the constraint, the constraint is always active and we have that the optimal FR capacity provision is:

$$r^* = \frac{\epsilon \cdot \sqrt{(\omega\tau)^2 + 1}}{A\ \ |K|}. \tag{5.12}$$

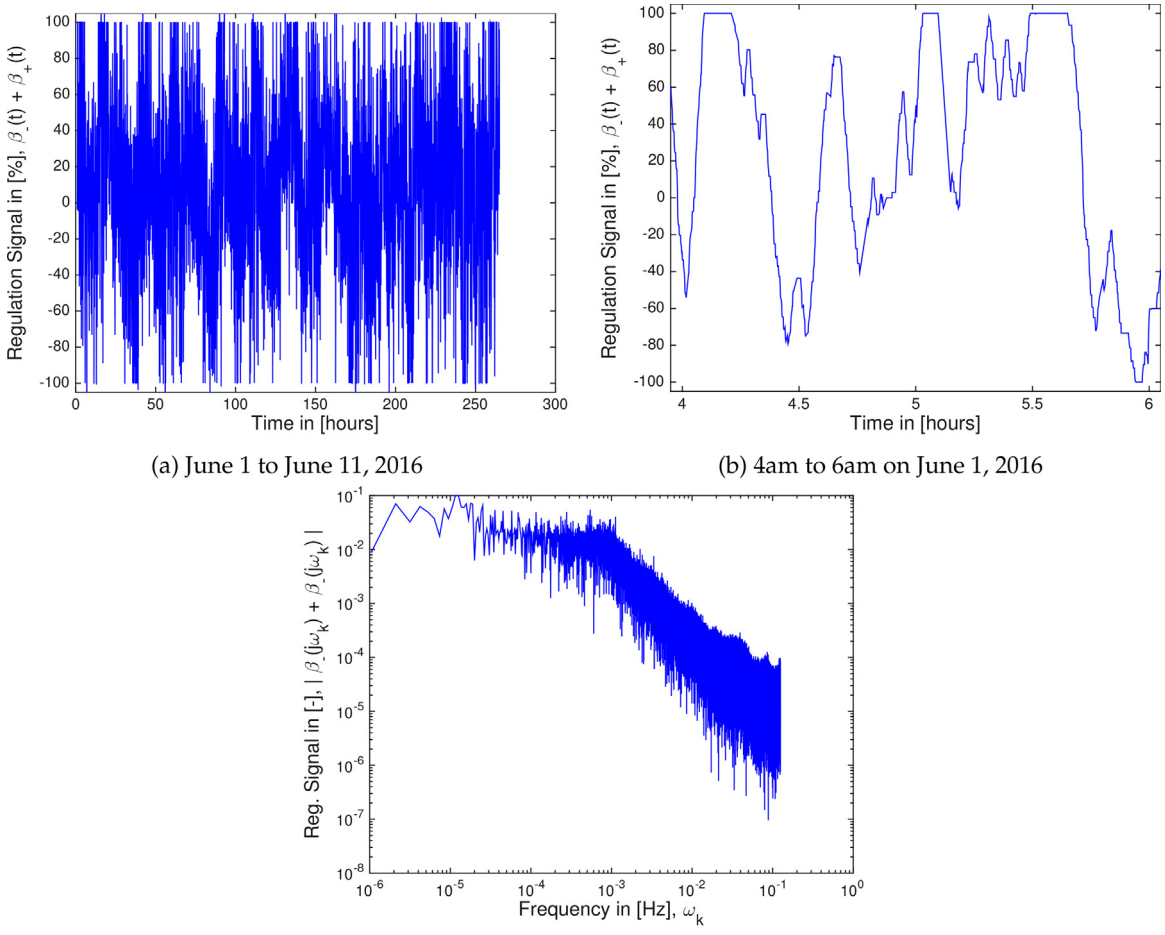

(a) June 1 to June 11, 2016

(b) 4am to 6am on June 1, 2016

(c) Power spectrum for June 1 to June 11, 2016

Fig. 5. System-wide FR dispatch signals and spectrum for ERCOT for June 1st–11th, 2016.

Consequently, the optimal revenue is:

$$\phi(r^*) = \frac{\pi \cdot \epsilon \cdot \sqrt{(\omega\tau)^2 + 1}}{A \quad |K|}. \tag{5.13}$$

As expected, the optimal revenue increases with increasing τ, decreases with increasing $|K|$, and increases with increasing flexibility margin ϵ. We express the optimal revenue as an implicit function of the flexibility $r^*(\epsilon)$ and we let α represent the maximum possible (ideal) FR capacity that can be collected by the system. The bound α is dictated by the system physical limits, such as the maximum electric load that it can use. Applying this bound to (5.12) gives the optimal FR capacity:

$$r^*(\epsilon) = \min\left(\frac{\epsilon \cdot \sqrt{(\omega\tau)^2 + 1}}{A \quad |K|},\ \alpha\right). \tag{5.14}$$

Note that, without this bound, (5.12) has the property that, as $A \to 0$, the system can provide unbounded FR capacity (i.e., $r^*(\epsilon) \to \infty$). This gives unrealistic revenues for hours with small (or no) FR dispatch. In contrast, (5.14) predicts $r^*(\epsilon) \to \alpha$ as $A \to 0$. It in convenient to expresses the FR capacity scaled by α:

$$\hat{r}^*(\epsilon) = \frac{r^*(\epsilon)}{\alpha}, \tag{5.15}$$

which indicates the fraction of available FR capacity that can be utilized. When $\hat{r}^*(\epsilon) < 1$, system dynamics limit participation in FR markets.

The optimal FR capacity can also be expressed as:

$$\hat{r}^*(\epsilon) = \min\left(\frac{\epsilon}{\alpha \cdot \max\limits_{t \in \mathcal{U}} |\hat{y}(t) - \bar{y}|},\ 1\right). \tag{5.16}$$

This representation is useful to evaluate FR revenues in the presence of more general FR dispatch signals that are composed of many frequencies such as (2.3). In particular, one can show that the maximum deviation of the UPR from steady-state is bounded as:

$$\max_{t \in \mathcal{U}} |\hat{y}(t) - \bar{y}| \leq |K| \sum_{k=0}^{N} \frac{\sqrt{A_k^2 + B_k^2}}{\sqrt{(\omega_k \tau)^2 + 1}}. \tag{5.17}$$

By combining (5.16) and (5.17), we can obtain an estimate of the optimal FR provision as:

$$\hat{r}^*(\epsilon) \approx \min\left(\frac{\hat{\epsilon}}{\sum_{k=0}^{N} \frac{\sqrt{A_k^2 + B_k^2}}{\sqrt{(\omega_k \tau)^2 + 1}}},\ 1\right), \tag{5.18}$$

where we define the dimensionless flexibility margin:

$$\hat{\epsilon} = \frac{\epsilon}{|K| \cdot \alpha}. \tag{5.19}$$

We note that this optimal FR provision estimate (5.18) can be computed explicitly (without any dynamic simulations) by using

the spectrum information of the FR signal and the parameters of the first-order system. One can compute an exact estimate of the optimal FR provision by explicitly computing the bound $\max_{t\in\mathcal{U}}|\hat{y}(t)-\bar{y}|$ through simulation of the UPR $\hat{y}(t)$ over $\mathcal{U}$. This approach, however, is computationally more expensive.

We use the FR provision estimate (5.18) to derive quick estimates of FR revenue for different first-order systems using historical market data from ERCOT. The dynamical system is fully characterized by the time constant τ and the dimensionless flexibility $\hat{\epsilon}$. We apply a Fourier expansion of the FR signal to obtain A_k, B_k and ω_k. For each hour in the data set, the FR revenue is computed from the provision estimate (5.18) and the prices $\pi_+(t)$, $\pi_-(t)$ from ERCOT. For hours with $\beta_+(t)-\beta_-(t)=0$, we define $\hat{r}^*=1$. The results are presented in Fig. 6. For a given time constant τ, the average hourly FR capacity provision approaches one as the flexibility $\hat{\epsilon}$ increases, as expected. The diminishing returns are explained by the variation in FR dispatch from hour-to-hour. As the flexibility budget $\hat{\epsilon}$ increases, $\hat{r}^*(\hat{\epsilon})$ reaches the saturation point. For a given flexibility budget $\hat{\epsilon}$, slower systems (those with larger τ) can provide greater FR capacity. This is because the amplitude of the UPR approaches zero as $\tau\to\infty$. From Fig. 6 we can also see that annual revenues predicted can *reach up to $140,000 for a system providing a single MW of FR capacity*.

5.2. Water–methanol distillation system

Previous studies reported in the literature have focused on providing FR services using energy systems with fast dynamics and large flexibility margins such as batteries, arc furnaces, aluminum smelters, buildings, pumps, and so on. We argue that many other energy-intensive unit operations having slow dynamics can also be used for providing FR capacity. To see this, we consider the distillation column system for an experimental binary water–methanol separation from Wood and Berry (1973):

$$\begin{bmatrix} x_D(j\omega) \\ x_B(j\omega) \end{bmatrix} = \begin{bmatrix} \dfrac{12.8e^{-j\omega}}{16.7(j\omega)+1} & \dfrac{-18.9e^{-3j\omega}}{21.0(j\omega)+1} \\ \dfrac{-6.6e^{-7j\omega}}{10.9(j\omega)+1} & \dfrac{-19.4e^{-3j\omega}}{14.4(j\omega)+1} \end{bmatrix} \begin{bmatrix} R(j\omega) \\ S(j\omega) \end{bmatrix} \tag{5.20}$$

The outputs $x_D(\cdot)$ and $x_B(\cdot)$ are the distillate and bottoms compositions (in wt% methanol), respectively. The input variables $R(\cdot)$ and $S(\cdot)$ are the reflux and steam flow rates (in lb/min), respectively. The time constants are expressed in minutes and we thus highlight that the system has a relatively slow response. The transfer functions (5.20) are built around deviations using the steady-state reference point $x_D=96.0$, $x_B=0.5$, $R=1.95$, $S=1.71$. We assume that the distillation system provides FR capacity by allowing variations in the energy input (steam) flow rate S. Consequently, the steam flow rate is treated as a disturbance. This can be realized in practice by either using an electric reboiler or by providing FR from a utility plant that supplies the steam. In the latter case, adjusting the electricity output of the utility plant to track the FR signal would also result in variations in steam flow rate that need to be absorbed by the distillation system. Wood and Berry report that the steam supply for their column is at 233.0 °C. Assuming that only the latent heat of vaporization is used, a 1.0 lb/min change in S is equivalent to a change of 956.6 Btu/min or 16.82 kW in the input energy flow rate. This is important, as hourly regulation prices are reported in $/MW. We set the FR capacity to $\alpha=11.5$ kW, which corresponds to a 40% deviation from the steady-state steam flow rate.

Table 2
Revenue estimates for distillation system from UPR analysis with historical ERCOT data.

Case	Variable	ϵ	$\hat{\epsilon}$	Avg. FR capacity	Annual revenue
A	x_D	0.1 wt%	7.7×10^{-3}	6.2%	8.62 $/kW
B	x_D	1.0 wt%	7.7×10^{-2}	59.8%	83.34 $/kW
C	x_B	0.1 wt%	7.5×10^{-3}	4.2%	6.03 $/kW

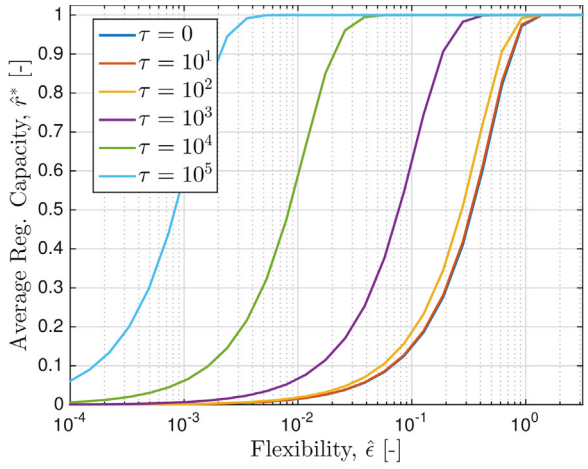

(a) FR Capacity

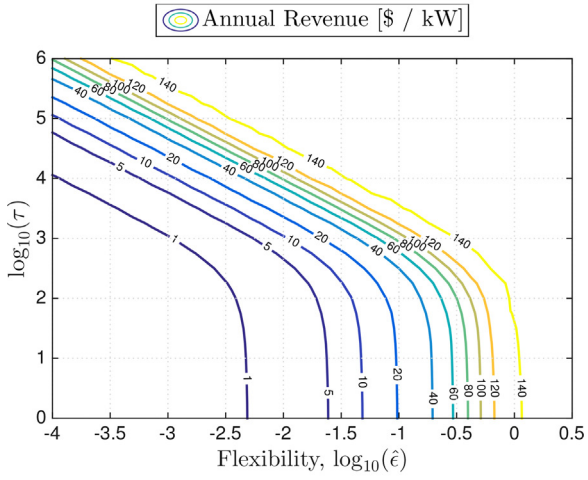

(b) Annual FR Revenue

Fig. 6. FR capacity allocations and revenues for first-order systems in ERCOT.

5.2.1. UPR analysis approach

In order to apply the previous analysis for linear systems, we neglect the time delay, and focus solely on the transfer functions relating S to x_D and x_B, and convert the units:

$$x_D(j\omega)=\frac{K_D}{\tau_D(j\omega)+1},\quad x_B(j\omega)=\frac{K_B}{\tau_B(j\omega)+1} \tag{5.21}$$

where $K_D=-1.12$ wt% per kW, $\tau_D=1.26\times10^3$ s, $K_B=-1.15$ wt% per kW, $\tau_B=8.64\times10^2$ s. We also highlight that the column is bench-scale with a nominal reboiler duty of 28.8 kW. Fig. 6 provides an estimate of potential FR market revenues obtained by using (5.18) on each individual transfer function separately (neglecting variable interactions). We begin by considering a flexibility margin of $\epsilon=1.0$ wt%, which corresponds to $\hat{\epsilon}\approx10^{-1}$. Fig. 6 predicts revenues near 80 $/kW. Table 2 shows results resulting from re-evaluating (5.18) with precise values for $\hat{\epsilon}$ corresponding to the distillation system. Fig. 7 shows the results along with three cases (labelled as

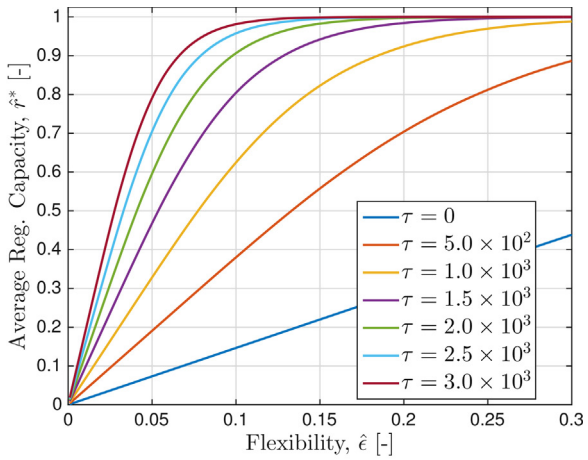

(a) Regulation Capacity

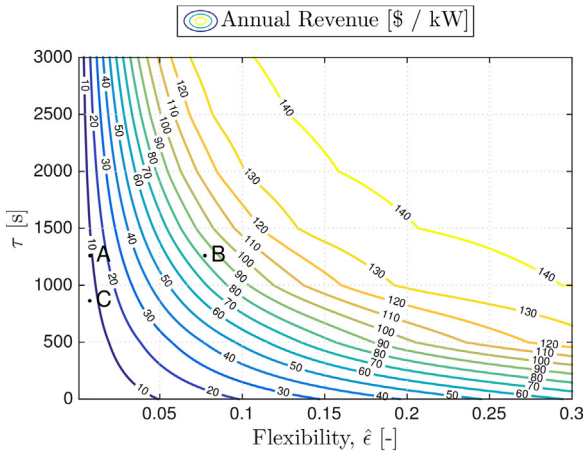

(b) Annual Revenues

Fig. 7. Optimal FR capacity provisions and revenues for distillation system (5.21) using UPR approach. Labels A, B, and C correspond to the cases in Table 2.

A, B, and C) from Table 2. For x_D, we see that an order of magnitude change in the flexibility ϵ (from 0.1 to 1.0 wt%) results in and order of magnitude change in revenues (8.6–83.3 $/kW).

Fig. 2 also offers interesting insights that can be used to guide the design of the distillation system. Consider the goal of capturing revenues of 127.5 $/ kW (which is 90% of available market revenues). With a flexibility of $\epsilon = 1.0$ wt% and K_D fixed, the time constant τ_D would need to be doubled. This can potentially be achieved by increasing material hold-ups. Alternatively, with τ_D fixed, K_D would need to be halved or ϵ would need to be doubled to 2.0 wt% to meet the 90% revenue goal.

5.2.2. Optimization approach

The UPR method provides rough estimates of potential FR revenue but is limited in that: (a) it considers flexibility budgets $\hat{\epsilon}$ in only one variable at a time (assuming decoupled dynamics), (b) it considers only open-loop responses (i.e., the reflux flow rate R is not used to counteract disturbances in the steam flow rate S), (c) the analysis uses the UPR trajectory to compute the regulation capacity but the system may not have enough time to settle, and (d) the formulation requires a prior specification of the ratio of FR up and down capacity provisions. To overcome these limitations, we use the more general optimization formulation (4.8). We consider a horizon of one hour (which matches pricing and bidding mechanisms for most day-ahead markets). The dynamics (4.8b) are discretized with four second timesteps to match the FR dispatch signal update rates. For the implementation of (5.20) in the time domain, we use a state-space representation of the form:

$$\mathbf{z}(t) = \mathbf{A}\ \ \mathbf{z}(t-1) + \mathbf{B}\begin{bmatrix} R(t) \\ S(t) \end{bmatrix},$$

$$\mathbf{y}(t) = \begin{bmatrix} x_D(t) \\ x_B(t) \end{bmatrix} = \mathbf{C}\ \ \mathbf{z}(t),$$

$$\mathbf{A} = \begin{bmatrix} 0.99602 & 0 & 0 & 0 \\ 0 & 0.9939 & 0 & 0 \\ 0 & 0 & 0.99683 & 0 \\ 0 & 0 & 0 & 0.99538 \end{bmatrix}, \tag{5.22}$$

$$\mathbf{B} = \begin{bmatrix} 0.066534 & 0 \\ 0.066463 & 0 \\ 0 & 0.066561 \\ 0 & 0.066513 \end{bmatrix},$$

$$\mathbf{C} = \begin{bmatrix} 0.76647 & 0 & -0.9 & 0 \\ 0 & 0.6055 & 0 & -1.3472 \end{bmatrix}.$$

The optimal FR capacity provision for a given hour is obtained by solving the discrete-time optimization problem:

$$\max_{\bar{S}, r_-, r_+, R} \ r_+ \cdot \pi_+ + r_- \cdot \pi_- + \rho \sum_{t \in \mathcal{T}} |R(t) - R(t-1)| \tag{5.23a}$$

$$\text{s.t. } \mathbf{z}(t) = \mathbf{A}\mathbf{z}(t-1) + \mathbf{B}\begin{bmatrix} R(t) \\ S(t) \end{bmatrix},\ t \in \mathcal{T}, \tag{5.23b}$$

$$\mathbf{y}(t) = \mathbf{C}\ \ \mathbf{z}(t),\ t \in \mathcal{T}, \tag{5.23c}$$

$$S(t) = r_+\beta_+(t) - r_-\beta_-(t) + \bar{S},\ t \in \mathcal{T}, \tag{5.23d}$$

$$\underline{\epsilon} \le \mathbf{y}(t) \le \bar{\epsilon},\ t \in \mathcal{T}, \tag{5.23e}$$

$$|R(t)| \le \delta,\ t \in \mathcal{T}, \tag{5.23f}$$

$$0 \le r_+,\quad r_- \le \alpha. \tag{5.23g}$$

The decision variables include the FR down capacity r_-, FR up capacity r_+, the steam flow rate offset $\bar{S}$, and the reflux flow rate $R(t)$ for $t \in \mathcal{T}$. The objective includes a term to penalize changes in the reflux flow rate to encourage gradual control actions and prevent wear-and-tear effects. Input parameters include the FR down and up prices (π_- and π_+), objective penalty ($\rho = 10^{-5}$), and FR up and down dispatch signals at each time step ($\beta_-(t)$ and $\beta_+(t)$). To improve scaling, the variables S, r_-, r_+, and α are expressed in lb/min in (5.23). A one-hour horizon includes T=900 time steps (one hour discretized using four-second timesteps) and we thus define the time set $\mathcal{T} = \{1, \ldots, T\}$ with $R(0) = 0$ and $\mathbf{z}(0) = \mathbf{0}$. Problem (5.23) contains 7202 variables with bounds, 5401 linear equality constraints, and 1801 linear inequality constraints.

Fig. 8 shows the optimal solution of (5.23) using market data from ERCOT, flexibility margins $\underline{\epsilon} = (-0.1, -0.1)$ and $\bar{\epsilon} = (0.1, 0.1)$ (in wt%), a bound on the reflux flow rate of $\delta = 0.78$ lb/min (which corresponds to 40% of the steady-state value) and a FR capacity bound $\alpha = 11.5$ (in kW). The dashed color lines indicate the steady-state values for each variable and the dotted black lines show bounds. For this hour, the optimal market provisions are $r_+^* = 1.2$ and $r_-^* = 3.4$ (in kW). This asymmetric FR capacity provisions stem from the higher price for FR down during this particular hour ($\pi_- = 3.98$ and $\pi_+ = 3.0$ in $/MW). The plots show that $x_D(t)$ and $x_B(t)$ hit their bounds, often more than once during the hour. This is because the optimizer is manipulating these profiles to maximize the FR revenues. The bounds on the steam flow rate $S(t)$ in Fig. 8d are not active in this hour. We also note that the system dynamics limit capacity provisions at this hour. Moreover, as the flexibility margins $\underline{\epsilon}$ and $\bar{\epsilon}$ are relaxed, the trajectories for the reflux flow rate $R(t)$ hit the bounds more often.

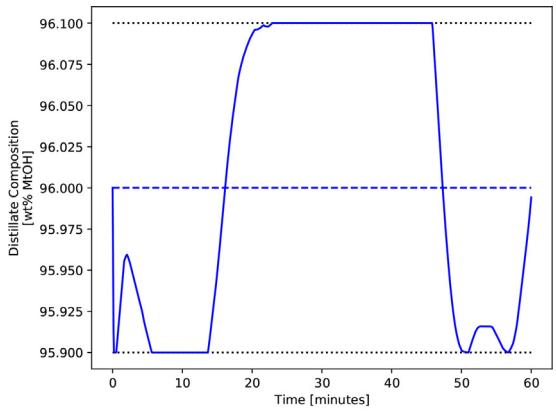

(a) Distillate Composition, $x_D(t)$

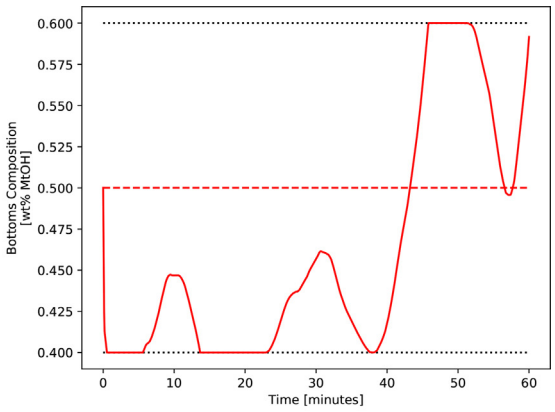

(b) Bottoms Composition, $x_B(t)$

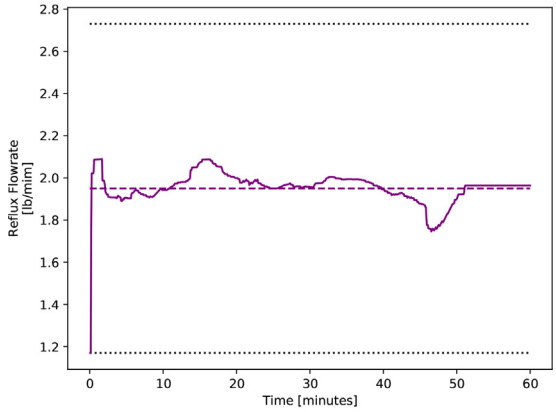

(c) Reflux Flow rate, $R(t)$

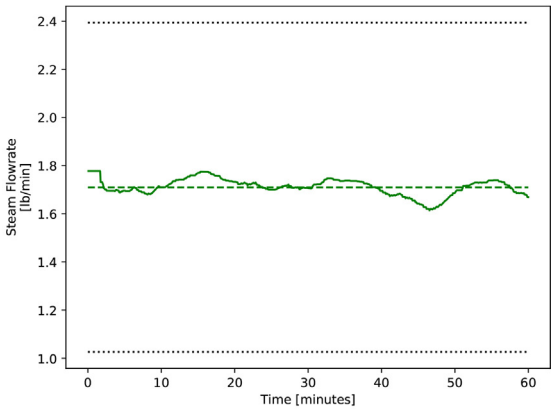

(d) Steam Flow rate, $S(t)$

Fig. 8. Results for (5.23) using ERCOT data for midnight to 1 am, July 1st, 2015.

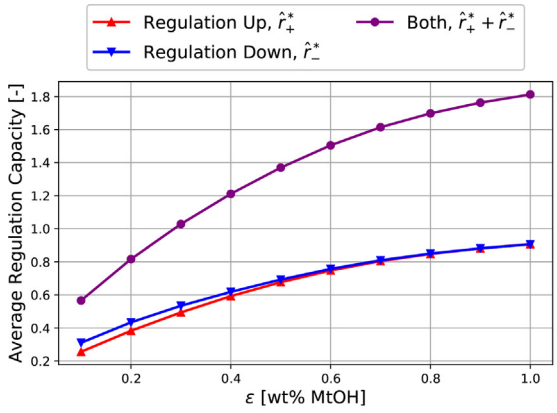

(a) Average Capacity Provisions

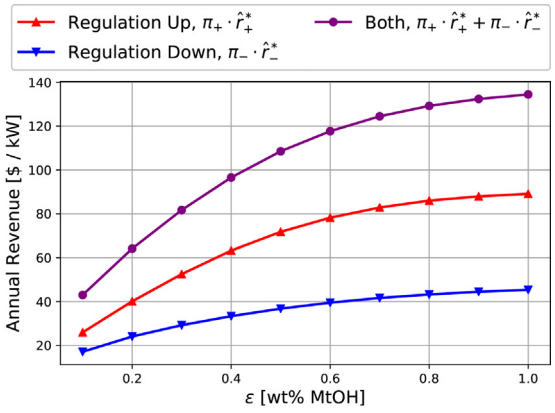

(b) Annual Revenue

Fig. 9. FR revenues as a function of flexibility for optimization approach.

To estimate revenues for an entire year we solve problem (5.23) for each hour. Here, flexibility margins were set to $\underline{\epsilon} = (-\epsilon, -0.1)$ and $\bar{\epsilon} = (\epsilon, \epsilon)$ in wt%. Fig. 9 shows the results for values of ϵ from 0.1 to 1.0 wt%. The lower bound for the deviation of x_B is fixed at -0.1 wt% to avoid negative compositions (non-physical solutions). As expected, there are strong improvements in revenues for additional flexibility. Notably, we notice that the maximum revenue predicted by the optimization approach is on the order of 140,000 $/MW, which is consistent with that obtained with the UPR approach.

Fig. 9a shows that, at $\epsilon = 0.1$ wt%, average FR capacity provisions are 26% (for up capacity) and 31% (for down capacity). By increasing

Table 3
Economic benefits of using reflux flow rate to counteract FR disturbance.

Flexibility	Adjust reflux R?	FR Capacity		Annual revenue
		Up	Down	
$\epsilon = 0.1$ wt%	No ($\delta = 0$ lb/min)	9.0%	13.9%	15.5 $/kW
	Yes ($\delta = 0.78$ lb/min)	25.6 %	31.0 %	43.0 $/kW
$\epsilon = 1.0$ wt%	No ($\delta = 0$ lb/min)	31.2%	40.8%	56.1 $/kW
	Yes ($\delta = 0.78$ lb/min)	90.7%	90.6%	134.5 $/kW

the flexibility margin to $\epsilon = 1.0$ wt% provisions increase to 91% for both up and down capacities. For the same flexibility margins, total revenues span 43,000–134,000 $/MW (see Fig. 9b). Interestingly, *average* FR provisions are almost identical for up and down products (see Fig. 9a). This is surprising given than the *average* price for FR up capacity (10.60 $/MW) is twice the *average* price from down capacity (5.57 $/MW). Intuitively, one would expect greater sales of the more valuable product. To further analyze this contradictory result, problem (5.23) was resolved for each hour for $\epsilon = 0.5$ wt% with r_- fixed to zero. With these restrictions, the optimal provisions are 83.4% for up capacity, giving 77.1 $/kW. In contrast, the optimization policy without the restriction sells 67.7% of up FR capacity for 71.8 $/kW and 69.2% of down FR capacity for 36.8 $/kW. Consequently, it is more lucrative to sell a blend of up and down FR capacities. This suggests that, although FR down capacity is twice as valuable as up capacity, it is also more difficult to provide. In other words, providing a unit of FR up capacity consumes a lesser amount of the total flexibility margin. Finally, it is important to note that the *average* FR capacities are nearly equal between up and down products, whereas the optimal ratio varies by hour depending on the price and FR dispatch signal. We also highlight that flexibility bands for the distillate and bottoms composition can potentially be expressed as average constraints, which can provide more flexibility.

Although the maximum possible FR revenues obtained with the the UPR and optimization approaches are similar, the UPR analysis of Section 5.2.1 predicted capacity provisions between 4% and 60% with revenues between 6,000 and 83,000 $/MW, whereas the optimization approach (Section 5.2.2) predicted capacity provisions between 26% and 91% with revenues between 43,000 and 134,000 $/MW. The difference is significant and stems from the assumptions used in the UPR technique. In particular, the UPR estimates neglect the ability to counteract the FR signal. In contrast, the optimization approach directly computes the best possible control strategy that mitigates the FR disturbance. To illustrate the effect of the additional flexibility gained with the control strategy, we solved (5.23) by setting $\delta = 0$ (which fixes the control $R(t) = 0$). The results, given in Table 3, indicate that the *control system can double to triple FR revenue*.

The $\delta = 0$ optimization cases facilitate direct comparison with the results of Table 2. For $\epsilon = 0.1$ wt%, UPR analysis predicts revenues of 6000 and 8000 $/MW, whereas the restricted optimization approach predicts 15,500 $/MW. The difference in this case arises because the latter approach can *adjust the blend of up and down FR capacity*. For $\epsilon = 1.0$ wt%, the UPR analysis predicts revenue of 83,300 $/MW, whereas the optimization formulation yields 56,000 $/MW. This difference is because the former (Case B) only consider bounds on the x_D trajectory, whereas the latter considers bounds on both x_D and x_B (including a tight lower bound on x_B). Consequently, the UPR approach overestimates performance.

Because the optimization formulation is more general and flexible, it is preferred for detailed economic assessment. On the other hand, the UPR technique can be used to quickly assess the impact of the time constant τ and flexibility $\hat{\epsilon}$ on revenue. The UPR analysis also involves simple calculations. For instance, all of the computations for Fig. 6 required less than 5 CPU-minutes in `Matlab`. In contrast, generating Fig. 9 for the optimization approach required the solution of 31,690 instances of (5.23), which took 8.5 hours for CPU time. Problem (5.23) was implemented in JuMP (Dunning et al., 2017) and solved with Gurobi 7.0.

To gain a perspective on the enormous *economic potential* for industrial-sized systems, we consider the following numbers. The annual methanol demand in 2015 was of around 70 million tonne per year, which was met by around 90 facilities world-wide.[2] This translates to an average methanol production of 33,000 lb/min per plant. Scaling-up the model of Wood and Berry (1973) suggests a nominal *steam demand of 800 MW for distillation in an average methanol plant*. Using only 1% of this energy input for FR in each direction ($\alpha = 8$ MW) could conservatively *result in revenues of 320,000 $/year* (computed from 40 $/kW/year $\times$ 8000 kW). Moreover, scaling up the production rate by a factor of 10^4 should slow down system dynamics (increase τ) and reduce the gain K (whose units are wt% per input energy). Both of these factors will increase the amount of FR capacity that can be sold. Thus the 40 $/kW/year estimated for the laboratory-scale column with $\epsilon = 0.1$ wt% is likely achievable with industrial size systems with a much tighter flexibility budget, as predicted by (5.19) and Fig. 6. The *maximum possible revenues for 8 MW of FR up and down capacity provided by the distillation system is in the order of 1.1 million $/year* (based on ECROT data for 2015 and 2016).

6. Conclusions and future directions

In this work, we have analyzed economic opportunities provided by frequency regulation (FR) markets to industrial systems. We use frequency domain analysis to highlight the dominant frequencies in FR dispatch signals and to argue that slow dynamical systems can naturally damp such frequencies. We propose a fast method to assess the FR revenue potential for open-loop dynamical systems and a more sophisticated optimization method to determine the maximum amount of FR provision that can be offered by a given industrial system while satisfying operational constraints. As part of future work, we are interested in accounting for uncertainty in prices and FR dispatch signals by using stochastic programming formulations and assessing the performance of different types of industrial-sized systems such as air separation units and cooling towers.

A limitation of implementing FR participation in industry is the potential wear and tear of actuation equipment at high frequencies (Hao et al., 2014). Consequently, it is necessary to design control architectures in a way that they only actuate on frequency spectra that is not too damaging to equipment while allowing the damaging spectra to be absorbed through natural damping. Existing low-level controllers are currently not capable of doing this (their sampling and actuation frequencies are high). Another issue is that, at high FR provision levels, it will be necessary to update the setpoint update frequency of real-time optimization layers. This will need a closer integration of real-time optimization and supervisory control layers (e.g., through economic MPC) (Biegler and Zavala, 2009; Rawlings et al., 2012). It is thus necessary to re-think sampling, update, and actuation intervals for different levels real-time optimization, supervisory, and low-level control.

Acknowledgments

We thank the Vice Chancellor for Research and Graduate Education at the University of Wisconsin-Madison and the industrial members of the TWCCC consortium for the generous support.

[2] http://www.methanol.org/the-methanol-industry.

References

Al-Mansour, F., Kožuh, M., 2007. Risk analysis for CHP decision making within the conditions of an open electricity market. Energy 32 (10), 1905–1916.

Ashok, S., 2006. Peak-load management in steel plants. Appl. Energy 83 (5), 413–424.

Ashok, S., Banerjee, R., 2001. An optimization mode for industrial load management. IEEE Trans. Power Syst. 16 (4), 879–884.

Babatunde, A.O., Ray, W.H., 1994. Process Dynamics, Modeling and Control. Oxford University Press.

Babu, C.A., Ashok, S., 2008. Peak load management in electrolytic process industries. IEEE Trans. Power Syst. 23 (2), 399–405.

Baccino, F., Conte, F., Massucco, S., Silvestro, F., Grillo, S., 2014. Frequency regulation by management of building cooling systems through model predictive control. Power Systems Computation Conference (PSCC), 1–7.

Biegler, L.T., Zavala, V.M., 2009. Large-scale nonlinear programming using ipopt: an integrating framework for enterprise-wide dynamic optimization. Comput. Chem. Eng. 33 (3), 575–582.

Cao, Y., Swartz, C.L., Baldea, M., Blouin, S., 2015. Optimization-based assessment of design limitations to air separation plant agility in demand response scenarios. J. Process Control 33, 37–48.

Cao, Y., Swartz, C.L.E., Flores-Cerrillo, J., 2016. Optimal dynamic operation of a high-purity air separation plant under varying market conditions. Ind. Eng. Chem. Res. 55 (37), 9956–9970.

Castro, P.M., Harjunkoski, I., Grossmann, I.E., 2009. New continuous-time scheduling formulation for continuous plants under variable electricity cost. Ind. Eng. Chem. Res. 48, 6701–6714.

Castro, P.M., Harjunkoski, I., Grossmann, I.E., 2011. Optimal scheduling of continuous plants with energy constraints. Comput. Chem. Eng. 35 (2), 372–387.

Castro, P.M., Sun, L., Harjunkoski, I., 2013. Resource-task network formulations for industrial demand side management of a steel plant. Ind. Eng. Chem. Res. 52 (36), 13046–13058.

Christidis, A., Koch, C., Pottel, L., Tsatsaronis, G., 2012. The contribution of heat storage to the profitable operation of combined heat and power plants in liberalized electricity markets. Energy 41 (1), 75–82.

Coatalem, M., Mazauric, V., Pape-Gardeux, C.L., Maïzi, N., 2017. Optimizing industries' power generation assets on the electricity markets. Appl. Energy 185 (Part 2), 1744–1756.

Cusset, B.F., Mellichamp, D., 1975. On-line identification of process dynamics. A multi-frequency response method. Ind. Eng. Chem. Process Des. Dev. 14 (4), 359–368.

Daryanian, B., Bohn, R., Tabors, R., 1989. Optimal demand-side response to electricity spot prices for storage-type customers. IEEE Trans. Power Syst. 4 (3), 897–903.

De Paepe, M., Mertens, D., 2007. Combined heat and power in a liberalised energy market. Energy Convers. Manag. 48 (9), 2542–2555.

Dowling, A.W., Kumar, R., Zavala, V.M., 2017. A multi-scale optimization framework for electricity market participation. Appl. Energy 190, 147–164.

Dunning, I., Huchette, J., Lubin, M., 2017. Jump: a modeling language for mathematical optimization. SIAM Rev. 59 (2), 295–320.

2013. Table 11.1 Electricity: Components of Net Demand 2010. Technical report. U.S. Energy Information Administration, pp. 3.

Everett, G., Philpott, A., 2002. Pulp electricity demand management. Proceedings of the 37th Annual Conference of Operations Research Society of New Zealand, vol. 5, 5–63.

Fares, R.L., Meyers, J.P., Webber, M.E., 2014. A dynamic model-based estimate of the value of a vanadium redox flow battery for frequency regulation in Texas. Appl. Energy 113, 189–198.

Feng, J., Brown, A., O'Brien, D., Chmielewski, D.J., 2015. Smart grid coordination of a chemical processing plant. Chem. Eng. Sci. 136, 168–176, Control and Optimization of Smart Plant Operations.

Hao, H., Lin, Y., Kowli, A.S., Barooah, P., Meyn, S., 2014. Ancillary service to the grid through control of fans in commercial building HVAC systems. IEEE Trans. Smart Grid 5 (4), 2066–2074.

Hao, H., Middelkoop, T., Barooah, P., Meyn, S., 2012. How demand response from commercial buildings will provide the regulation needs of the grid. 50th Annual Allerton Conference on Communication, Control, and Computing, 1908–1913.

Ierapetritou, M.G., Wu, D., Vin, J., Sweeney, P., Chigirinskiy, M., 2002. Cost minimization in an energy-intensive plant using mathematical programming approaches. Ind. Eng. Chem. Res. 41, 5262–5277.

Karwan, M.H., Keblis, M.F., 2007. Operations planning with real time pricing of a primary input. Comput. Oper. Res. 34 (3), 848–867.

Kirby, B., O'Malley, M., Ma, O., Cappers, P., Corbus, D., Kiliccote, S., Onar, O., Starke, M., Steinbergy, D., 2011. Load Participation in Ancillary Services (Workshop Report). Technical Report December. U.S. Department of Energy.

Lin, Y., Barooah, P., Meyn, S., Middelkoop, T., 2015. Experimental evaluation of frequency regulation from commercial building HVAC systems. IEEE Trans. Smart Grid 6 (2), 776–783.

Meyn, S., Barooah, P., Busic, A., Ehren, J., 2013. Ancillary service to the grid from deferrable loads: the case for intelligent pool pumps in Florida. In: IEEE 52nd Annual Conference on Decision and Control (CDC), IEEE, pp. 6946–6953.

Mitra, S., Grossmann, I.E., Pinto, J.M., Arora, N., 2012. Optimal production planning under time-sensitive electricity prices for continuous power-intensive processes. Comput. Chem. Eng. 38, 171–184.

Mitra, S., Sun, L., Grossmann, I.E., 2013. Optimal scheduling of industrial combined heat and power plants under time-sensitive electricity prices. Energy 54, 194–211.

Mullin, R., 2016, June. CAISO regulation costs quadruple as prices, procurement jump. RTO Insider.

Pattison, R.C., Touretzky, C.R., Johansson, T., Harjunkoski, I., Baldea, M., 2016. Optimal process operations in fast-changing electricity markets: framework for scheduling with low-order dynamic models and an air separation application. Ind. Eng. Chem. Res. 55 (16), 4562–4584.

Rawlings, J.B., Angeli, D., Bates, C.N., 2012. Fundamentals of economic model predictive control. In: IEEE 51st Annual Conference on Decision and Control (CDC), IEEE, pp. 3851–3861.

Rong, A., Lahdelma, R., 2007. Efficient algorithms for combined heat and power production planning under the deregulated electricity market. Eur. J. Oper. Res. 176 (2), 1219–1245.

Todd, D., 2013. They Said It Couldn't Be Done: Alco's Experience in Demand Response. Texas Industrial Energy Management Forum: Energy Management in the Age of Shale Gas, Houston, TX.

Todd, D., Caufield, M., Helms, B., Starke, M., Kirby, B., Kueck, J., 2009. Providing Reliability Services through Demand Response: A Preliminary Evaluation of the Demand Response Capabilities of Alcoa Inc. Technical report. Alcoa Power Generating, Inc., Oak Ridge National Laboratory, ORNL/TM-2008/233.

Vujanic, R., Mariéthoz, S., Goulart, P., Morari, M., 2012. Robust integer optimization and scheduling problems for large electricity consumers. In: American Control Conference (ACC), IEEE, pp. 3108–3113.

Walling, R.A., 2008. Analysis of Wind Generation Impact on ERCOT Ancillary Services Requirements. Technical Report. GE Energy.

Wood, R., Berry, M., 1973. Terminal composition control of a binary distillation column. Chem. Eng. Sci. 28 (9), 1707–1717.

Zhang, Q., Grossmann, I.E., 2016. Enterprise-wide optimization for industrial demand side management: fundamentals, advances, and perspectives. Chem. Eng. Res. Des. 116, 114–131.

Zhang, Q., Cremer, J.L., Grossmann, I.E., Sundaramoorthy, A., Pinto, J.M., 2016a. Risk-based integrated production scheduling and electricity procurement for continuous power-intensive processes. Comput. Chem. Eng. 86, 90–105.

Zhang, Q., Morari, M.F., Grossmann, I.E., Sundaramoorthy, A., Pinto, J.M., 2016b. An adjustable robust optimization approach to provision of interruptible load by continuous industrial processes. Comput. Chem. Eng. 86, 106–119.

Zhang, X., Hug, G., 2014, July. Optimal regulation provision by aluminum smelters. IEEE PES General Meeting | Conference Exposition, 1–5.

Zhang, X., Hug, G., 2015, February. Bidding strategy in energy and spinning reserve markets for aluminum smelters' demand response. IEEE Power Energy Society Innovative Smart Grid Technologies Conference (ISGT), 1–5.

Zhang, Q., Grossmann, I.E., Heuberger, C.F., Sundaramoorthy, A., Pinto, J.M., 2015a. Air separation with cryogenic energy storage: optimal scheduling considering electric energy and reserve markets. AIChE J. 61 (5), 1547–1558.

Zhang, X., Hug, G., Kolter, Z., Harjunkoski, I., 2015, October. Industrial demand response by steel plants with spinning reserve provision. North American Power Symposium (NAPS), 1–6.

Zhao, P., Henze, G.P., Brandemuehl, M.J., Cushing, V.J., Plamp, S., 2015. Dynamic frequency regulation resources of commercial buildings through combined building system resources using a supervisory control methodology. Energy Build. 86, 137–150.

Zhao, P., Henze, G.P., Plamp, S., Cushing, V.J., 2013. Evaluation of commercial building HVAC systems as frequency regulation providers. Energy Build. 67, 225–235.

Zhou, D., Zhou, K., Zhu, L., Zhao, J., Xu, Z., Shao, Z., Chen, X., 2017. Optimal scheduling of multiple sets of air separation units with frequent load-change operation. Sep. Purif. Technol. 172, 178–191.

Zhu, Y., Legg, S., Laird, C.D., 2011. A multiperiod nonlinear programming approach for operation of air separation plants with variable power pricing. AIChE J. 57 (9), 2421–2430.